Accurate American Option Pricing by Grid Stretching and High Order Finite Differences

Cornelis W. Oosterlee *, Coenraad C.W. Leentvaar [1], Xinzheng Huang

Delft Institute of Applied Mathematics (DIAM), Delft University of Technology, the Netherlands.

Abstract

In this paper, we present an accurate discretization for the numerical solution of the Black-Scholes equation for pricing European options and for the linear complementarity problem related to pricing American options. The aim is to find accurate option prices and hedge parameters with a small number of grid points. Fourth order finite differences are employed, as well as a grid stretching in space by means of an analytic coordinate transformation. This transformation is made time-dependent for pricing American options following the optimal exercise boundary. Numerical pricing experiments including discrete dividend payment confirm the accuracy of the methods proposed.

Key words: option pricing, Black-Scholes, fourth order finite differences, grid transformation, American option, discrete dividend, time-dependent stretching

1 Introduction

In option pricing an accurate representation of the Greeks or hedge parameters, i.e., the derivatives of the option prices, is at least as important as the option price itself. This is because an instantaneously risk-free portfolio typically consists of options and a number, Delta, of shares. If the value of the

* corresponding author

Email addresses: c.w.oosterlee@math.tudelft.nl (Cornelis W. Oosterlee), c.c.w.leentvaar@math.tudelft.nl (Coenraad C.W. Leentvaar), x.huang@ewi.tudelft.nl (Xinzheng Huang).

[1] This author wants to thank the Dutch Technology Foundation (STW) for financial support

shares decreases, the option's value should increase proportionally. Delta is related to the first derivative of the option price with respect to the share price. Risk neutrality of a portfolio is one of the main goals in option pricing.

The aim in this paper is to provide an efficient and accurate discretization for obtaining option values and the Greeks for European and for American style options. For European options the reference equation is the Black-Scholes equation. For American options, where early exercise is allowed, it is a linear complementarity problem, with constraints, that needs to be solved. Here the accurate determination of the time-dependent optimal exercise share price is another topic of research. A realistic market feature, the discrete dividend payment once or twice a year, is included in the discussion and in the numerical experiments. Some option pricing background is presented in Section 2. The reader is referred to the basic literature [6,8,12,13] for detailed information.

Grid accuracy is pursued by means of grid stretching and fourth order finite difference discretizations. In order to cluster grid points in the region of interest, i.e., near the option's exercise price and the initial share price, an analytic grid transformation, as in [1,10] is applied. A transformation modifies all coefficients in the equation, but discretization can take place on an equidistant grid. Fourth order finite differences in space and time are then chosen for discretizing this transformed equation. The transformation is adapted in a time-dependent way to deal with American options. The grid transformation is described in Section 3; the discretization in Section 4. For plain vanilla European options, closed form solutions exist [6,12]. They serve here as a reference for the numerical option prices and Greeks. Since the Greeks are often obtained by a numerical differentiation the accuracy of these derivatives is not obvious beforehand. Theoretically, numerical differentiation reduces the accuracy by one order. These are, however, statements on the asymptotic behavior for grid size tending to zero. With the highly accurate discretizations, however, we expect a reasonable accuracy of the hedging parameters.

In [11] a comparison of different methods for computing hedge parameters of an American call was performed. The advanced Leisen Reimer binomial tree method produced the most satisfactory results. The finite difference method evaluated in [11], however, was rather basic, based on second order finite differences in space and the Crank-Nicolson time discretization on an equidistant grid. Oscillations were then encountered in various parameters in [11]. Here, the hedge parameters are computed on coarse stretched grids with the fourth order discretization. Numerical option pricing experiments are presented in Section 5. We focus on the application of the numerical techniques. It is not trivial to set up rigorous theory for the methods developed for the option pricing problems on the coarse grids of interest.

2 Option Pricing Basics

2.1 Plain Vanilla European Options

Two widely traded option contracts are European put and call options. With a European put option, the holder of the option may sell shares at the expiration date for the exercise price. The other party of the option contract, the writer, must buy the shares, if the holder decides to sell them. With a European call option, the holder has the right to purchase shares at the expiration date for a prescribed amount. The writer is then obliged to sell the shares.

The basic equation in option pricing is the Black-Scholes partial differential equation (PDE). The value u of a European option depends on share price s and is influenced by exercise price K, time t to maturity T ($0 \le t < T$), interest rate r, and volatility σ:

$$\frac{\partial u}{\partial t} + \mathcal{L}u := \frac{\partial u}{\partial t} + \frac{1}{2}\sigma^2 s^2 \frac{\partial^2 u}{\partial s^2} + (r - r_d)s\frac{\partial u}{\partial s} - ru = 0, \quad 0 \le s < \infty, \quad 0 \le t < T \ . \tag{1}$$

Here, a continuous dividend payment r_d (modeled as some ratio of the share price) is included. This is a satisfactory model for, e.g., index options. It is replaced by a discrete dividend payment for options on a single share. Equation (1) is valid under the assumption of a geometric Brownian motion for the underlying share price process $\{S_t\}$. More advanced models, based on jump-diffusion processes, local or stochastic volatility are not considered here. However, as the resulting operators for option pricing with those models may contain a Black-Scholes part, the discretization outlined here may be of some interest there as well.

The equation comes with boundary and final conditions distinguishing a put from a call option. Boundary conditions arise naturally from financial arguments: The boundary condition for a put, see, for example [6,12], at $s = 0$ is $u(0,t) = Ke^{-r(T-t)}$. It represents the exponential discounting for receiving an amount K at $t = T$ with constant interest rate r. Furthermore, $u(s,t) \to 0$ as $s \to \infty$, because one obviously cannot gain by exercising the put option. The payoff at maturity is known and determines the final condition at $t = T$. For a European put, it reads:

$$u(s,T) := \Phi(s) = \max(K - s, 0). \tag{2}$$

The left boundary condition for a call is $u(0,t) = 0$ for all t, and a choice for the right-side boundary condition for $s \to \infty$ is $u(s,t) = se^{-r_d(T-t)} - Ke^{-r(T-t)}$. These boundary conditions can also be deduced from the *put-call*

parity relation [6]. For a European call, the final condition reads:

$$u(s,T) := \Phi(s) = \max(s-K,0). \tag{3}$$

2.2 American Style Options

In contrast to European options, which can only be exercised at the maturity date T, American options can be exercised at any time up to T. Consequently, identifying the optimal exercise strategy is an integral part of the valuation problem.

Let $u(t,s)$ be the value of an American option with payoff $\Phi(s)$ (2), (3) at exercise. The possibility of early exercise requires

$$u(t,s) \geq \Phi(s), \quad \forall\, t \in [0,T],$$

otherwise an arbitrage opportunity would arise [6,12,13].

The valuation of the American option is known as a free boundary problem. The free boundary share price $s_f(t)$, also called optimal exercise boundary or early exercise boundary, divides the (t,s) half strip into two parts, namely the continuation region and the stopping region. The continuation region $\{(t,s) \in [0,T] \times \mathbb{R}_+ : u(t,s) > \Phi(s)\}$ is the set of points (t,s) at which the option is worth more alive, while in the stopping region $\{(t,s) \in [0,T] \times \mathbb{R}_+ : u(t,s) = \Phi(s)\}$ early exercise is advisable.

Therefore under the Black-Scholes framework, the price $u(t,s)$ satisfies either in the continuation region

$$u(t,s) > \Phi(s), \quad \frac{\partial u}{\partial t} + \frac{1}{2}\sigma^2 s^2 \frac{\partial^2 u}{\partial s^2} + (r - r_d)s\frac{\partial u}{\partial s} - ru = 0;$$

or in the stopping region

$$u(t,s) = \Phi(s), \quad \frac{\partial u}{\partial t} + \frac{1}{2}\sigma^2 s^2 \frac{\partial^2 u}{\partial s^2} + (r - r_d)s\frac{\partial u}{\partial s} - ru < 0.$$

Additionally, the boundary conditions at $s_f(t)$ are that u and $\partial u/\partial s$ are continuous at $s_f(t)$:

$$u(t, s_f(t)) = \Phi(s_f(t)), \quad \frac{\partial u(t, s_f(t))}{\partial s} = \Phi'(s_f(t)),$$

known as the *smooth fit principle*.

This leads to a *linear complementarity problem* formulated as follows

$$u(t,s) \geq \Phi(s), \tag{4}$$

$$-\Big(\frac{\partial u}{\partial t} + \frac{1}{2}\sigma^2 s^2 \frac{\partial^2 u}{\partial s^2} + (r - r_d)s\frac{\partial u}{\partial s} - ru\Big) \geq 0, \tag{5}$$

$$\Big(\frac{\partial u}{\partial t} + \frac{1}{2}\sigma^2 s^2 \frac{\partial^2 u}{\partial s^2} + (r - r_d)s\frac{\partial u}{\partial s} - ru\Big)\Big(u(t,s) - \Phi(s)\Big) = 0 \tag{6}$$

with final and boundary conditions. The optimal exercise boundary $s_f(t)$ is automatically captured by this formulation and can be determined a-posteriori. Solutions of linear complementarity problems can be obtained by a variety of iterative methods, e.g., by the projected successive overrelaxation (PSOR) [2] method we are to use.

2.3 American Options and Discrete Dividend

We examine in this section the early exercise boundary of American puts with discrete dividend. The case of an American call with discrete dividends is easier than the put and we refer to [8].

Consider an American put under the Black-Scholes framework with strike K and maturity T. Suppose a dividend is to be paid at time t_d and t_d^-, t_d^+ represent the times just before and after the dividend date, respectively. It is known that in $[0, t_d^-)$ and $[t_d^+, T)$ the value $u(t,s)$ is the solution of the Black-Scholes equation. Therefore from time t_d^+ to T, the optimal exercise boundary behaves like that of a non-dividend paying American put. From the no-arbitrage principle, the option price must be continuous across the instant of discrete dividend, i.e.,

$$u(t_d^-, s_{t_d^-}) = u(t_d^+, s_{t_d^+}). \tag{7}$$

Moreover the underlying share will drop by the same amount as the dividend right after the payment, i.e., $s_{t_d^+} = f(s_{t_d^-})$, where $f(s) = (1-\rho)s$ if the dividend is paid at a fixed rate ρ, or $f(s) = s - D$ if the dividend is paid at a fixed amount D.

The holder of a deep in-the-money American put would tend to defer exercise until t_d^+ in order to benefit from the decrease in the price of the underlying share after dividend payment. Hence, $s_f(t_d^-) = 0$.

Let us first consider the case of fixed dividend rate ρ. Assume we have a portfolio consisting of a stock s and a put option u. At some time prior to the dividend date $t = t_d - \delta t$, one encounters the following situation: If one exercises the option the interest income from t to t_d is $Ke^{r\delta t}$; if one holds the option and exercises immediately after the dividend payment, say at t_d^+, the

gain is $K + \rho s_{t_d^-}$, which is stochastic up to time t. The free boundary $s_f(t)$ is determined by matching the profit in the risk neutral world (with probability measure Q) from the two strategies. With a fixed dividend rate ρ this leads to

$$K[e^{r\delta t} - 1] = \rho E^Q[s_{t_d^-}|\mathcal{F}_t] = \rho e^{r\delta t} s_f(t) = \rho e^{r\delta t}[s_f(t) - s_f(t_d^-)], \tag{8}$$

with E being the expectation. Taking the limit $\delta t \to 0$ one finds

$$\lim_{t \to t_d^-} s_f'(t) = -rK/\rho. \tag{9}$$

In the case of fixed dividend amount D, the gain of the above portfolio changes to $K + D$ if we exercise the option at t_d^+. Early exercise is not optimal if

$$Ke^{r\delta t} < K + D, \tag{10}$$

which indicates that the early exercise boundary will disappear for a period of

$$\delta t = \ln(1 + D/K)/r \tag{11}$$

before the ex-dividend date t_d. These general properties of options under discrete dividend will be verified in the numerical experiments in Section 5.

In order to calculate option prices and the option's derivatives we use advanced numerical techniques, based on classical concepts.

3 Grid Transformation

With a simple transformation, $\tau = T - t$, the equation that is backward in time is changed into an equation forward in time. Minus signs are added at the appropriate places in the equation. In the notation, however, we keep t instead of τ.

3.1 Spatial Grid, Fixed Grid Stretching (FS)

The accuracy of a finite difference approximation depends on the existence of several derivatives in the Taylor's expansion, but in option pricing the final condition is not differentiable (or even discontinuous in the case of a digital option). Therefore, local grid refinement seems a logical choice to retain a satisfactory accuracy. It is well-known that local grid refinement near sharp corners in the domain or near singularities in an equation often improves the overall discretization accuracy drastically. By an h-refinement in the vicinity

of a singularity the discretization error is locally decreased, due to the smaller h, and the global accuracy is not spoiled by the well-known *pollution effect*, as it is encountered for elliptic or parabolic equations. The principle of local refinement is simple: Place more points in the neighborhood of the grid points where the non-differentiable condition occurs. This can be done by adaptive grid refinement for some regions, based on an error indicator, or by an *analytic coordinate transformation*, which results in an a-priori stretching of the grid. A coordinate transformation is the most elegant way in our applications as the region of interest is known beforehand. An equidistant grid discretization can be used after the analytic transformation, as only the coefficients in front of the derivatives change. We explain the principle for a general parabolic PDE with non-constant coefficients, Dirichlet boundary conditions and an initial condition:

$$\frac{\partial u}{\partial t} = \alpha(s)\frac{\partial^2 u}{\partial s^2} + \beta(s)\frac{\partial u}{\partial s} + \gamma(s)u(s,t) \tag{12}$$

$$u(a,t) = L(t), \quad u(b,t) = R(t), \quad u(s,0) = \phi(s). \tag{13}$$

Consider a coordinate transformation $y = \psi(s)$, which must be one-to-one, with inverse $s = \varphi(y) = \psi^{-1}(y)$ and let $\hat{u}(y,t) := u(s,t)$ (unknowns with "hat" live on the transformed grid). By the chain rule, the first and second derivative with respect to s of $u(s,t)$ will become:

$$\frac{\partial u}{\partial s} = \frac{\partial \hat{u}}{\partial y}\frac{dy}{ds} = \frac{\partial \hat{u}}{\partial y}\left(\frac{ds}{dy}\right)^{-1} = \frac{1}{\varphi'(y)}\frac{\partial \hat{u}}{\partial y}, \tag{14}$$

$$\frac{\partial^2 u}{\partial s^2} = \left(\frac{ds}{dy}\right)^{-1}\frac{\partial}{\partial y}\left(\left(\frac{ds}{dy}\right)^{-1}\frac{\partial \hat{u}}{\partial y}\right) = \frac{1}{(\varphi'(y))^2}\frac{\partial^2 \hat{u}}{\partial y^2} - \frac{\varphi''(y)}{(\varphi'(y))^3}\frac{\partial \hat{u}}{\partial y}. \tag{15}$$

Application of (14) and (15) to (12) changes the factors α, β and γ into:

$$\widehat{\alpha}(y) = \frac{\alpha(\varphi(y))}{(\varphi'(y))^2}, \quad \widehat{\beta}(y) = \frac{\beta(\varphi(y))}{\varphi'(y)} - \alpha(\varphi(y))\frac{\varphi''(y)}{(\varphi'(y))^3}, \quad \widehat{\gamma}(y) = \gamma(\varphi(y)). \tag{16}$$

The boundary points a and b are also transformed into $\psi(a)$ and $\psi(b)$, respectively. The equidistant grid size for the transformed equation is $h = (\psi(b) - \psi(a))/N$, assuming function ψ to be a monotonically increasing function.

The spatial transformation used for Black-Scholes equation here is not new. It originates from [1] and is also presented in [10]:

$$y = \psi(s) = \frac{\sinh^{-1}(\xi\,(s-\kappa)) - c_1}{c_2 - c_1}, \tag{17}$$

with normalization constants $c_1 = \sinh^{-1}(\xi(a-\kappa))$ and $c_2 = \sinh^{-1}(\xi(b-\kappa))$, so that $y \in [0,1]$. The grid is refined around $s = \kappa$, which is typically set to K.

Parameter ξ determines the rate of stretching. In the analytic function (17) the combination $\xi\kappa$ appears. For satisfactory accuracy, especially on coarse grids, it appears advantageous to keep this quantity constant. $\xi\kappa = 15$, for example, has proven to be an appropriate choice over a variety of option pricing parameters. Figure 1 shows the stretching around $\kappa = 15$ for $\xi = 1$ ($\xi\kappa = 15$) and $\xi = 12$ ($\xi\kappa = 180$) and a corresponding grid. The difference in the number of points per s-interval with $\xi = 1$ and $\xi = 12$ is depicted in Figure 2. The number of points per interval is displayed for three grid sizes of 20-, 40- and 80 points with different colors (from light to dark in Fig. 2). Thus, larger ξ means fewer points in the outer regions. When ξ decreases the grid approaches an equidistant one.

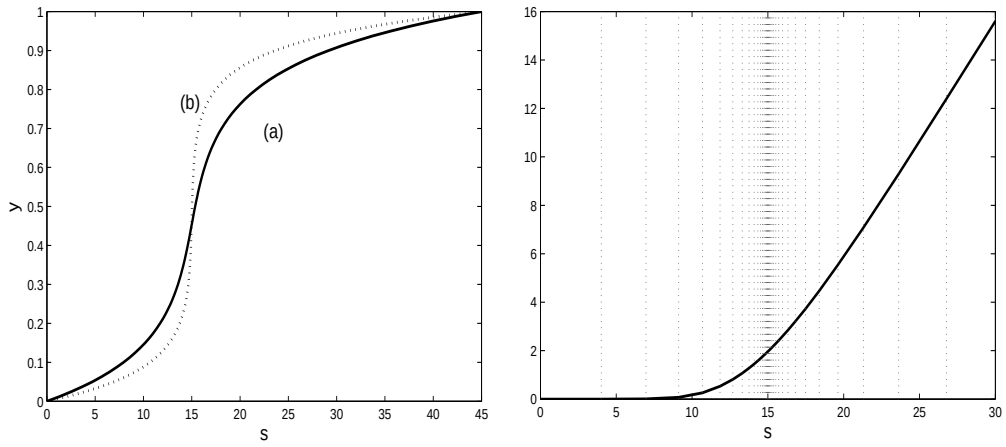

Fig. 1. Left: Transformation function (17), $\kappa = 15$, (a): $\xi = 1$, (b): $\xi = 12$; Right: Example of European call option values on the stretched grid.

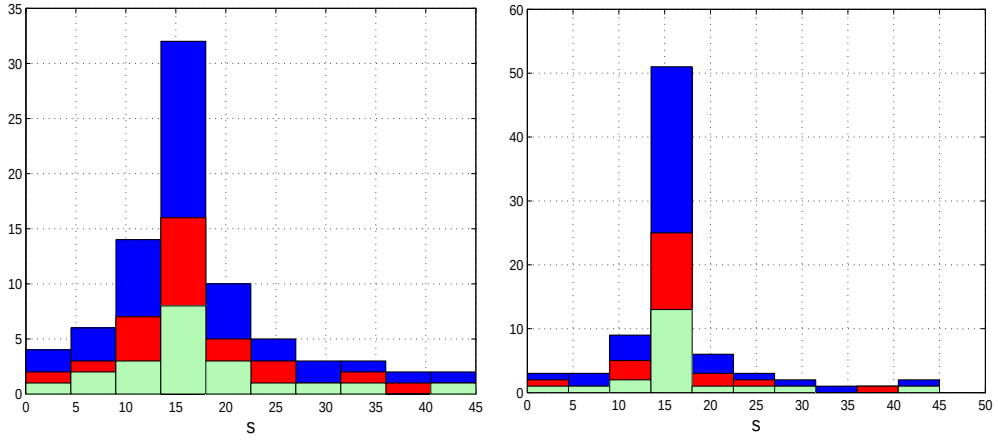

Fig. 2. Number of grid points in an interval on s-axis for $\xi = 1$ (left) and $\xi = 12$ (right). The number of points is 20, 40 and 80 for the colors from light to dark.

For transformation (17), the inverse and the first two derivatives are:

$$\varphi(y) = \frac{1}{\xi}\sinh\left(c_2 y + c_1(1-y)\right) + \kappa, \tag{18}$$

$$J(y) = \frac{c_2 - c_1}{\xi}\cosh\left(c_2 y + c_1(1-y)\right), \tag{19}$$

$$H(y) = \frac{(c_2 - c_1)^2}{\xi}\sinh\left(c_2 y + c_1(1-y)\right). \tag{20}$$

Here $J(y)$, the Jacobian, is the first derivative of $\varphi(y)$ and $H(y)$, the Hessian, denotes its second derivative. Applying transformation (18) to the final condition gives:

$$\hat{u}(y,T) = \max\left(\frac{1}{\xi}\sinh\left(c_2 y + c_1(1-y)\right) + \kappa - K, 0\right). \tag{21}$$

The kink in the final condition of a European option does not disappear; the condition is not differentiable. This grid transformation around a fixed parameter κ is called "fixed grid stretching" (FS), here.

3.2 American Options, Time Dependent Grid Stretching (TS)

We now focus on the determination of the optimal exercise boundary for American options, $s_f(t)$. It is known that for an American call the free boundary $s_f(t)$ is a continuous, increasing function of time to maturity t.

In order to get an accurate $s_f(t)$ the grid need not necessarily be refined at strike K, but at $max(K, rK/r_d)$ for an American call and $min(K, rK/r_d)$ for an American put at $t = T$ [8]. Instead of choosing a fixed κ in transformation (17) for the whole duration of the option, we vary κ so that the grid is refined in the vicinity of the free boundary for all t. Notice that in option pricing with the Black-Scholes operator only at $t = T$ the solution (i.e., the payoff) contains a kink and thus requires refinement. It is not necessary for accuracy reasons to keep κ fixed at $\kappa = K$.

An accurate representation of the free boundary may be achieved by applying a *time-dependent grid stretching* (hereafter called TS). This handles especially well the case that the free boundary $s_f(t)$ runs out of the region of refinement of a fixed grid stretching (17), which often occurs in the case of long maturities and/or high volatilities. Since there is no tractable formula indicating how the free boundary $s_f(t)$ evolves with respect to time to maturity t, we simply propose to extract information on the free boundary $s_f(t)$ from a *predictor step*. This step is one computation with fixed grid stretching (FS) on a coarse grid. We then obtain an improved free boundary $s_f^{TS}(t)$ by a predictor-corrector type scheme:

(1) *Predictor*:

Apply FS with constant κ on a coarse grid (preprocessing step). We obtain $s_f^{FS}(t)$ and grid point $s_f^+(t)$, i.e., the point directly next to $s_f^{FS}(t)$ which satisfies $u(s_f^+) > \Phi(s_f^+)$.

(2) *Corrector*:

Apply TS with

$$\kappa(t) = \frac{1}{2}(s_f^{FS}(t) + s_f^+(t)).$$

So, the time-dependent $\kappa(t)$ is equal to the midpoint of $s_f^{FS}(t)$ and $s_f^+(t)$.

If one assumes the error of the finite difference method to be small enough and the inaccuracy in determining the free boundary coming from the spatial discretization, then for an American call $s_f^{FS}(t)$ is indeed an upper bound for the true free boundary and $s_f^+(t)$ is a lower bound. For the put it is vice versa. Choosing the midpoint as the center of the grid refinement is therefore a satisfactory compromise. In the discretization a time-dependent $\kappa(t)$ means that the coefficients $\widehat{\alpha}(y), \widehat{\beta}(y), \widehat{\gamma}(y)$ in (16) change each time step. The grid remains, however, equidistant.

4 Discretization in Space and Time

4.1 High Order Accuracy in Space

An equidistant y-grid remains after the transformation FS or TS, on which we apply high order discretization in space and in time. A fourth order "long stencil" finite difference discretization in space based on Taylor's expansion for (12),...,(17) is given by

$$\begin{aligned}\frac{\partial \hat{u}_i}{\partial t} &= \frac{1}{12h^2}\widehat{\alpha}_i\left(-\hat{u}_{i+2} + 16\hat{u}_{i+1} - 30\hat{u}_i + 16\hat{u}_{i-1} - \hat{u}_{i-2}\right) + \\ &+ \frac{1}{12h}\widehat{\beta}_i\left(-\hat{u}_{i+2} + 8\hat{u}_{i+1} - 8\hat{u}_{i-1} + \hat{u}_{i-2}\right) + \widehat{\gamma}_i\hat{u}_i + O(h^4), \quad 2 \le i \le N-2.\end{aligned} \tag{22}$$

Subscript i refers to grid point $y_i = ih$ on the transformed grid. First derivatives are discretized by central differences. This is an appropriate choice as long as the equation is not convection dominating. For the fourth order approximation, interior point y_1 needs a special treatment at the left-side boundary as well as point y_{N-1} at the right-side boundary.

An approach for the first (and last) grid point is to use backward or one-sided

differences, with difference scheme:

$$\frac{\partial \hat{u}_1}{\partial y} = \frac{-3\hat{u}_0 - 10\hat{u}_1 + 18\hat{u}_2 - 6\hat{u}_3 + \hat{u}_4}{12h} + \mathbf{O}(h^4), \tag{23}$$

$$\frac{\partial^2 \hat{u}_1}{\partial y^2} = \frac{10\hat{u}_0 - 15\hat{u}_1 - 4\hat{u}_2 + 14\hat{u}_3 - 6\hat{u}_4 + \hat{u}_5}{12h^2} + \mathbf{O}(h^4). \tag{24}$$

and similarly for y_{N-1}.

We also compute numerically two hedge parameters, Delta (Δ) and Gamma (Γ):

$$\Delta^s = \frac{\partial u}{\partial s}, \quad \Gamma^s = \frac{\partial^2 u}{\partial s^2} \ . \tag{25}$$

Δ is an important parameter in hedging with options (as mentioned in the introduction). It is a measure of the rate of change in the option price with respect to the price of the underlying share. Γ measures the rate of change in the option's delta with respect to the share price. With a fourth order accurate scheme, we find

$$\Delta_i^y = \frac{\partial \hat{u}}{\partial y} = \frac{-\hat{u}_{i+2} + 8\hat{u}_{i+1} - 8\hat{u}_{i-1} + \hat{u}_{i-2}}{12h}, \tag{26}$$

$$\Gamma_i^y = \frac{\partial^2 \hat{u}}{\partial y^2} = \frac{-\hat{u}_{i+2} + 16\hat{u}_{i+1} - 30\hat{u}_i + 16\hat{u}_{i-1} - \hat{u}_{i-2}}{12h^2}. \tag{27}$$

On the s-grid the approximate derivatives read (14),(15):

$$\Delta_i^s = \left(\frac{d\varphi}{dy}\right)_i^{-1} \Delta_i^y, \quad \Gamma_i^s = \left(\frac{d\varphi}{dy}\right)_i^{-2} \Gamma_i^y - \left(\frac{d^2\varphi}{dy^2}\right)_i \left(\frac{d\varphi}{dy}\right)_i^{-3} \Delta_i^y. \tag{28}$$

4.2 Time Grid

We aim for an implicit discretization of fourth order on an equidistant grid in time with time step k. A well-known family of implicit schemes with nice properties is the family of backward differentiation formulae, BDF, of which the $\mathbf{O}(k^2)$ BDF2 [3,4] is known best. The $O(k^4)$-scheme, BDF4, is the basis for the time discretization employed. It reads

$$\left(\frac{25}{12}I - kL\right) u^{j+1} = 4u^j - 3u^{j-1} + \frac{4}{3}u^{j-2} + \frac{1}{4}u^{j-3}, \tag{29}$$

with k the time step, I the identity matrix, L a discrete version of $\mathcal{L}$ (1). Superscript j on discrete unknown u^j represents the iteration index in time.

This method needs three initialization steps. The combination of two Crank-Nicolson and one BDF3 step ($O(k^3)$) form the initialization for BDF4 here.

BDF2 is known to be unconditionally stable, whereas BDF3 and BDF4 have stability regions. For our applications so far, however, the stability constraints are not problematic.

4.3 Grid Stretching and Discrete Dividend

We adopt the technique of modeling discrete dividend by a jump condition at the ex-dividend date t_d (7). As mentioned, t_d^-, t_d^+ represent the times just before and after the ex-dividend date, respectively. The following numerical procedure is applied: We first perform a Black-Scholes computation until the ex-dividend date. This is done with the stretched grid transformation and the fourth order discretizations in space and in time. At the ex-dividend date, (7) is taken into account by means of interpolation. Accurate interpolation at this date on the stretched grid is an important feature, since typically $s_{t_d^+}$ (7) may not be a grid point. Lagrange interpolation of 4th order has been applied, to accurately implement the jump condition. After the ex-dividend date the Black-Scholes computation is restarted with the initialization by two Crank-Nicolson steps and the BDF3 step preceding the BDF4 iterations in time. In our computations we place t_d exactly on a time line, t_d^- and t_d^+ are assumed to lie on the same line. In [5] a modification to avoid negative share prices for a dividend payment of the form $s - D$ is proposed, especially for D large. Due to the grid stretching we have the largest mesh sizes at the boundaries of the computational domain. Therefore, even with relatively large dividend payments $s - D$ will often remain positive. The modification from [5] avoiding negative share prices after the ex-dividend date is thus not necessary here, although it would be straightforward to implement. A reference test from [5] is chosen to evaluate the performance of the finite difference method on coarse grids.

In the case of American options and discrete dividend we have indicated in Section 2.3 that the free boundary may disappear for some time. The strategy with the time-dependent $\kappa(t)$ is that we follow the free boundary, as soon as it appears, until the ex-dividend date with the predictor-corrector scheme from Section 3.2. At the ex-dividend date the free boundary may disappear. We then refine around $s = 0$ until the free boundary reappears. After the reappearance we continue to follow the free boundary with the predictor-corrector scheme.

5 Numerical Results

5.1 European Vanilla Call

The first numerical experiment is related to a European option with parameters: $K = 15,\ \sigma = 0.3,\ r = 0.05,\ r_d = 0.03,\ T = 0.5$. The plain vanilla call is computed to gain some insight in the properties of the numerical techniques. The numerical solution, its first and second derivatives at initial time t_0 are compared to the analytic solution in the infinity norm [2]. Next to this, the tables below present the error reduction factors c_∞, defined as:

$$c_\infty = \frac{\|w_{2h} - w_{ex}\|_\infty}{\|w_h - w_{ex}\|_\infty},$$

for a some vector w, where w_h, w_{2h} and w_{ex} denote the solutions on mesh size $h, 2h$ and the exact solution, respectively. We aim for accuracy with only a small number of grid points, therefore the grids are typically not finer than 80×80 points. The outer boundary s_{max} has been placed at 3 times the exercise price, according to the formula in [7].

Table 1 presents results obtained on an *equidistant* grid for a second order scheme ($O(h^2)$ finite differences and Crank-Nicolson) and the fourth order discretization (22). The second order scheme is the basis for many of the existing Black-Scholes based software. It is shown in Table 1 that second order accuracy is indeed achieved on these coarse equidistant grids, whereas the fourth order method is not performing better than second order. This is due to the lack of smoothness of the final condition. The convergence of the Greeks is also satisfactory.

Table 2 shows results on *stretched* grids with the second and fourth order discretization with $\xi = 1$. Stretching is fixed (FS) around $\kappa = K$ ($\xi\kappa = 15$). The accuracy of the results in u_h, Δ_h and Γ_h is nicely improved, especially for the fourth order discretization. We do not observe a 4th order error reduction on these coarse moderately stretched grids, but the error for 20×20 points is already less than one cent (€ 0.01) with the transformation. This is a very satisfactory result.

The asymptotic fourth order convergence rate is observed for larger values of ξ, i.e., with a severe stretching around the kink in the payoff. Table 3 confirms

[2] The use of the *relative error* was suggested. However, this is not suitable for measuring the global accuracy, as $u_{ex} \to 0$, for $s \to 0$. An alternative represents the *point-wise* relative error $|(u_h - u_{ex})/u_{ex}|$, for example, at $s = K$. The convergence of the price and Greeks measured in the relative error is very similar to the results for the absolute error and thus omitted.

Table 1
Comparison of error and accuracy in u_h, Δ_h and Γ_h $(t = 0)$ on equidistant grids.

Scheme	Grid	$\|u_h - u_{ex}\|_\infty$	c_∞	$\|\Delta_h - \Delta_{ex}\|_\infty$	c_∞	$\|\Gamma_h - \Gamma_{ex}\|_\infty$	c_∞
	10×10	1.3×10^{-1}		9.7×10^{-2}		2.1×10^{-2}	
$\mathbf{O}(h^2 + k^2)$	20×20	3.3×10^{-2}	4.0	9.6×10^{-3}	10.1	6.2×10^{-3}	3.4
	40×40	6.4×10^{-3}	5.2	1.7×10^{-3}	5.6	1.9×10^{-3}	3.3
	10×10	9.4×10^{-2}		3.0×10^{-2}		1.9×10^{-2}	
$\mathbf{O}(h^4 + k^4)$	20×20	1.6×10^{-2}	6.1	9.9×10^{-3}	3.0	3.1×10^{-3}	6.3
	40×40	4.1×10^{-3}	3.8	1.2×10^{-3}	8.2	3.6×10^{-4}	8.5

Table 2
Comparison of error and accuracy in u_h, Δ_h and Γ_h at t_0 on the stretched grid, $\xi = 1$.

Scheme	Grid	$\|u_h - u_{ex}\|_\infty$	c_∞	$\|\Delta_h - \Delta_{ex}\|_\infty$	c_∞	$\|\Gamma_h - \Gamma_{ex}\|_\infty$	c_∞
	10×10	6.6×10^{-2}		1.1×10^{-1}		8.5×10^{-3}	
$\mathbf{O}(h^2 + k^2)$	20×20	1.8×10^{-2}	3.8	2.6×10^{-2}	4.0	3.7×10^{-3}	2.3
	40×40	4.3×10^{-3}	4.1	6.5×10^{-3}	4.0	8.5×10^{-4}	4.3
	10×10	1.1×10^{-2}		2.4×10^{-2}		6.3×10^{-3}	
$\mathbf{O}(h^4 + k^4)$	20×20	1.1×10^{-3}	10.0	3.1×10^{-3}	7.6	1.3×10^{-3}	4.8
	40×40	9.4×10^{-5}	11.2	2.9×10^{-4}	10.8	9.7×10^{-5}	13.6

this for the option value u_h and $\xi = 12$. The convergence for Δ_h and Γ_h is also satisfactory. However, the error on the coarser grids with $\xi = 12$ is significantly larger than that obtained for $\xi = 1$ in Table 2. This justifies the suggested condition $\xi\kappa = 15$. The stretched grid, the solution and Greeks for $\xi = 1$ and $\xi = 12$ are displayed in Figure 3.

Table 3
Comparison of error and accuracy in u_h, Δ_h and Γ_h at t_0 on the stretched grid, $\xi = 12$.

Scheme	Grid	$\|u_h - u_{ex}\|_\infty$	c_∞	$\|\Delta_h - \Delta_{ex}\|_\infty$	c_∞	$\|\Gamma_h - \Gamma_{ex}\|_\infty$	c_∞
	10×10	2.7×10^{-1}		1.7×10^{-1}		4.2×10^{-2}	
$\xi = 12$	20×20	1.5×10^{-2}	18.1	1.5×10^{-2}	11.5	4.2×10^{-3}	10.0
stretching	40×40	9.1×10^{-4}	16.5	1.7×10^{-3}	8.6	5.3×10^{-4}	8.0
$\mathbf{O}(h^4 + k^4)$	80×80	5.7×10^{-5}	16.0	1.5×10^{-4}	11.6	4.2×10^{-5}	12.7
	160×160	3.7×10^{-6}	15.1	1.2×10^{-5}	12.4	4.2×10^{-6}	9.6

5.1.1 European Option, Discrete Dividend

Next, we present a result for a European call with multiple discrete dividend payments during the contract period, as in [5], and parameters $s_0 = K = 100, r = 0.06, \sigma = 0.25$, and multiple dividends of $D = 4$. The ex-dividend date is each half year. We choose again $s_{max} = 3K$ according to [7]; the stretching parameter is set to $\xi = 0.15$ (so that $\xi\kappa = \xi K = 15$).

Table 4 presents numerical results for $T = 1$, $T = 2$ and $T = 3$, with one, two and three dividend payments, respectively. It compares the numerical approximation to the exact solution from [5] (HHL in the table). For larger values of T the number of points in time increases proportionally. The numerical results obtained with a small number of grid points are very satisfactory. They compare very well with the reference results.

Table 4
Multiple discrete dividends payments, $K = 100, D = 4, \xi = 0.15$.

	$T = 1$		$T = 2$		$T = 3$
Grid	u_h $(t = 0)$	Grid	u_h $(t = 0)$	Grid	u_h $(t = 0)$
10×10	10.612	10×20	15.178	10×30	18.699
20×20	10.660	20×40	15.202	20×60	16.607
40×40	10.661	40×80	15.201	40×120	18.600
80×80	10.661	80×160	15.201	80×240	18.600
HHL	10.661		15.199		18.598

5.2 American Style Options

In this section we give three numerical examples. We consider an American call with a continuous dividend, American puts with discrete dividend and an American butterfly spread.

5.2.1 American Call With Continuous Dividend

An American style option test has been presented in [11]. In the test the continuous dividend r_d is set such that a free boundary appears for the American call. Results were obtained on extremely fine grids with 1130 grid points in spatial and time-wise directions. The results with finite differences in [11] were not completely convincing. The evaluation has been performed with the

following set:

$$K = 0.9, \quad r = 0.02, \quad r_d = 0.035, \quad T = 0.25. \tag{30}$$

We aim for satisfactorily accuracy in 40 - 80 grid points in both directions, first with $\sigma = 0.1$. With $K = 0.9$ we set the stretching parameter $\xi = 16$ in (17); the outer boundary is placed at $3K$. The option price converges on the stretched grid in fewer than 32 grid points; on the equidistant grid convergence is obtained in about 64 grid points. The convergence of the American option price (not shown) is very similar to the European counterpart.

To assess the accuracy of the methods proposed for computing the free boundary $s_f(t)$, we choose a 640 points reference grid in spatial and time-wise directions with FS, $\kappa = K = 0.9$ and $\xi = 16$ as our benchmark. The error measure we report is Root Mean Square(RMS) absolute error, defined by

$$RMS = \sqrt{\frac{1}{m}\sum_{t=\Delta t}^{m\Delta t}(s_f(t) - s_f^{REF}(t))^2}, \quad where\ m = T/\Delta t$$

and $s_f^{REF}(t)$ is the free boundary from the very fine benchmark grid.

Figure 4 compares the results obtained on a fixed stretched (FS) and on a time-dependent stretched grid (TS) to those obtained on an equidistant grid. Although it is obvious that the stretched grid gives far better approximations than the equidistant grid, we get only crude step functions for $s_f(t)$ with 40-80 grid points.

Remark: Unlike the computation of option prices, when the objective is to find an accurate approximation of $s_f(t)$, we pursue local accuracy. The condition $\xi\kappa = 15$ can then be relaxed in the corrector step. By choosing a large ξ , we can calculate $s_f^{TS}(t)$ on a grid that would cluster almost all grid points in the region of interest. Experiments show that this further improves the determination of $s_f(t)$ in the test case considered.

We further point out that the gain of TS strongly depends on the volatility σ. Table 5 presents the RMS in $s_f(t)$ for different σ. We again adopt the parameters in (30) and vary σ from 0.05 to 0.4. ξ is fixed at 16. TS is more advantageous as σ increases: the RMS errors are reduced significantly when $\sigma = 0.2 - 0.4$. Figure 4 (lower figures) shows that when $\sigma = 0.4$ the accuracy in $s_f(t)$ from an 80 point TS-grid is nearly comparable to that of a 320 point FS-grid. Whereas when σ is as small as 0.05, the accuracy from 80 points FS is already satisfactory and the improvement in accuracy from TS is negligible. This is in accordance with our expectations.

We now consider the Greeks Δ_h and Γ_h with the set from (30). Volatility σ is chosen to be $\sigma = 0.1$ and $\sigma = 0.4$. For $\sigma = 0.1$ the hedge parameters obtained

Table 5
Comparison of RMS error in $s_f(t)$ with different σ, $\xi = 16$.

σ	80 points FS	80 points TS	320 points FS
0.05	2.3×10^{-3}	2.2×10^{-3}	5.4×10^{-4}
0.1	2.8×10^{-3}	2.0×10^{-3}	7.0×10^{-4}
0.2	5.0×10^{-3}	1.9×10^{-3}	1.3×10^{-3}
0.3	7.7×10^{-3}	2.4×10^{-3}	2.0×10^{-3}
0.4	1.1×10^{-2}	4.1×10^{-3}	2.8×10^{-3}

on *equidistant* grids with 40^2 to 320^2 points (in space and time) are presented in Figure 5. Δ_h is not accurate for 40 equidistant points, so Γ_h with 40 points is not displayed. Γ_h is not yet resolved well with 80 equidistant grid points. For $\sigma = 0.4$ similar results are found.

The results on a fixed stretched grid, FS, are more favorable especially for the small volatility $\sigma = 0.1$, see figure 6. We focus on Γ_h, which is well captured on an 80 point grid with a fixed stretching. On the 40 point grid both Greeks are well resolved except maybe at the free boundary.

Improved accuracy in the hedge parameters near the early exercise boundary $s_f(T)$, especially in Γ_h, which is discontinuous at $s_f(T)$, is achieved by the application of the time-dependent stretching TS. Again, TS is more powerful when σ is large (here, when $\sigma = 0.4$). The improvements in the accuracy of Γ_h on an 80 point grid with $\sigma = 0.1$ and $\sigma = 0.4$ are shown in Figure 6.

Another issue for the accurate representation of Γ_h near the early exercise boundary is to use one-sided and backward differences, as in (23),(24), that do not need values across the free boundary. This way one can avoid local overshoots in Γ_h at the free boundary.

We finally mention that also the other Greeks, Rho ($\partial u/\partial r$), Vega ($\partial u/\partial \sigma$), Volga ($\partial^2 u/\partial \sigma^2$) and Vanna ($\partial^2 u/\partial s \partial \sigma$) have been computed on stretched grids varying from 40^2 to 320^2 points. In [11] uneconomical oscillations were observed in these Greeks for second order finite differences on coarse equidistant grids. Here, we did not observe any uneconomical oscillation in either of these Greeks, not even on grids with only 40 points.

5.2.2 American Put With Discrete Dividend

Now, we consider an American put option pricing problem with discrete dividend. The numerical results obtained with a fixed dividend payment $D = 0.02$ are in accordance with the analytic results from (11): The period that the free boundary disappears $\delta t \approx 0.2475$ with parameters $K = 1$, $r = 0.08$, $r_d =$

0, $T = 0.5$, $t_d = 0.3$, $\sigma = 0.4$ and this period remains constant for varying σ. Figure 7a presents the free boundary for a fixed dividend payment, and compares a reference boundary obtained on a fine 320 points mesh with results obtained by 80 point grids with FS and TS. The 80 point TS-grid solution coincides with the fine reference grid. The result with FS is also satisfactory. Figure 7b compares the numerical results for a dividend *rate* $\rho = 0.02$ with FS and TS 80 point grids with a fine reference grid. As shown in Figure 7b, FS gives stairs as a representation of the free boundary when the free boundary drops to 0 at t_d and remains outside of the region of its refinement, while TS generates a curve with exactly the slope as given by (9). TS is certainly the better choice in this situation. In either case, the discrete dividend payment does not pose any specific problems and TS improves the accuracy of the free boundary well. We further show how the s-grid evolves in time under TS in Figure 7c and 7d. Each dot in the graph represents a time-spatial grid point.

5.2.3 American Butterfly Spread

A butterfly option has the payoff $(S-K_1)^+ + (S-K_2)^+ - 2(S-K_3)^+$, which can be thought of as a portfolio consisting of a long position in two calls with strikes K_1 and K_2 respectively and a short position in two calls with the middle strike $K_3 = (K_1 + K_2)/2$.

For the numerical solution of an American butterfly, we stretch the grid at the three strike prices, where the payoff is not smooth. This is achieved by defining a global Jacobian that combines the individual Jacobians for each strike price. Following [10], we use the harmonic squared average for the combination, which yields a smooth transformation:

$$J(y) = A\left[\sum_{k=1}^{n} J_k(y)^{-2}\right]^{-\frac{1}{2}}, \text{ where } \quad J_k(y) = \left[(\frac{1}{\xi_k})^2 + (\varphi_k(y) - \kappa_k)^2\right]^{\frac{1}{2}}. \quad (31)$$

Here, A is a normalization constant that must be calculated iteratively. At each stretching position, the global Jacobian $J(y)$ is dominated by the behavior of the local $J_k(y)$. The global transformation $s = \varphi(y)$ is then obtained by numerically integrating the global Jacobian.

The position that needs extra care during discretization is the vicinity of K_3. To avoid any interference between the numerical solutions on grid points that lie at different sides of K_3, we choose second order three-point discretization stencils for the direct neighboring grid points of K_3:

$$\frac{\partial \hat{u}_i}{\partial y} = \frac{\hat{u}_{i+1} - \hat{u}_{i-1}}{2h} + \mathbf{O}(h^2), \quad \frac{\partial^2 \hat{u}_i}{\partial y^2} = \frac{\hat{u}_{i+1} - 2\hat{u}_i + \hat{u}_{i-1}}{h^2} + \mathbf{O}(h^2). \quad (32)$$

Figure 8 shows the option prices at $t = 0$ and the corresponding grid with parameters $K_1 = 0.5$, $K_2 = 1.5$, $\sigma = 0.1$, $r = 0.02$, $r_d = 0.015$, $T = 3$. The grid has now three refinement positions: K_1, K_2 and K_3. With this set of parameters we observe the occurrence of two free boundaries, one lies left of K_3 and one right, see Figure 8.

We note that it is possible to employ TS to improve the accuracy of the two free boundaries as demonstrated in Figure 8. However, if with TS a new numerically transformed grid is generated at each time step, it is time-consuming compared to the analytic transformation and significantly degrades the speed of the program. This is due to the iterative solver for A and the numerical integration for the s-grid. However, it may not be necessary to update the grid each time step. After the predictor step, it can be decided whether or not to update the grid at a time step.

6 Conclusions

In this paper we have solved European and American option pricing problems with a small number of grid points. Fourth order accurate space and time discretizations have been employed, using spatial grid stretching by means of an analytical coordinate transformation. With parameters that give a severe grid stretching, fourth order accuracy can be obtained for European options. Important for our applications is, however, a small discretization error with only a few grid points. This is achieved by the techniques proposed and a moderate grid stretching. For the European reference problem, 20 to 40 space- and time-steps are sufficient to get an accuracy of less than one cent (€ 0.01). Furthermore, we have observed a satisfactory accuracy of the hedge parameters.

For pricing American options we proposed a time-dependent grid stretching in a predictor-corrector type scheme. The predictor step finds a crude approximation of the free boundary on a coarse (fixed) stretched grid; The corrector step applies the time-dependent stretching based on the results in the predictor step. The Greeks can then be accurately resolved by 80 grid points. The optimal exercise boundary is also well captured by 80 grid points. Options on shares paying discrete dividends are handled very satisfactorily by the stretched grid discretization and a 4th order Lagrange interpolation at the ex-dividend date. The time-dependent stretching refines at share price 0 if the free boundary disappears. A more complicated strategy, like an American butterfly option, can also be handled well within this framework.

The scheme proposed can be generalized to higher dimensional problems. In summary, we do not see any reason for not recommending finite differencing on stretched grids for solving option pricing problems numerically.

References

[1] N. Clarke, K. Parrot, Multigrid for American option pricing with stochastic volatility, *Appl. math. finance,* 6:177-179, 1999.

[2] C.W. Cryer, The solution of a quadratic programming problem using systematic overrelaxation, *SIAM J. Control* 9: 385-392, 1971.

[3] C.W. Gear, *Numerical initial value problems for ordinary differential equations.* Prentice-Hall, Englewood Cliffs NJ, 1971.

[4] E. Hairer, K. Wanner, *Solving ordinary differential equations. Vol. 2. Stiff and differential-algebraic problems.* Springer Verlag, Heidelberg, 1996.

[5] E.G. Haug, J. Haug and A. Lewis, Back to basics: a new approach to the discrete dividend problem. *Wilmott Magazine,* 37-47, Sept 2003.

[6] J.C. Hull, *Options, futures and other derivatives,* Prentice-Hall Int. Inc, London, 1989.

[7] R. Kangro, R Nicolaides, Far field boundary conditions for Black-Scholes equations, *SIAM J. Numerical Analysis,* 38(4): 1357-1368, 2000.

[8] Y.K. Kwok, *Mathematical models of financial derivatives.* Springer Verlag, Heidelberg, 1998.

[9] G.H. Meyer, Numerical investigation of early exercise in American puts with discrete dividends, *J. Comp. Finance,* 5(2), Winter 2001/02.

[10] D. Tavella, C. Randall, *Pricing financial instruments, the finite difference method.* Wiley New York, 2000.

[11] C. Wallner and U. Wystrup, Efficient computation of option price sensitivities for options of American style. *Wilmott Magazine* 2-11, November 2004.

[12] P. Wilmott, S. Howison, J. Dewynne, *The mathematics of financial derivatives,* Cambridge University Press, Cambridge, 1997.

[13] P. Wilmott, *Paul Wilmott introduces quantitative finance*, Wiley 2001.

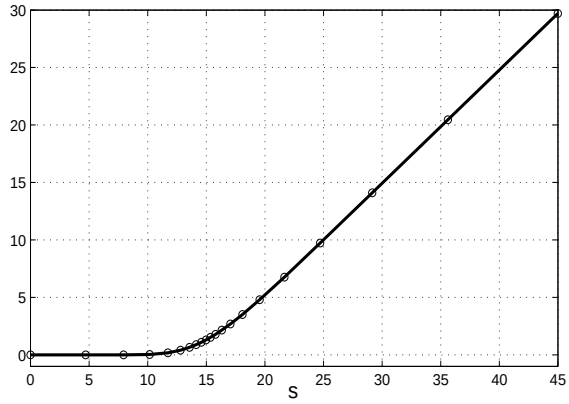

(a) $u_h,\ \xi = 1$

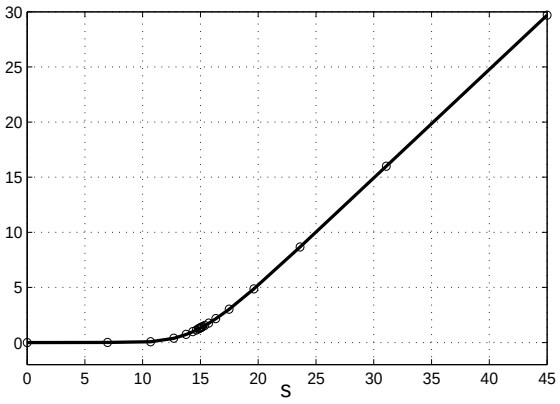

(b) $u_h,\ \xi = 12$

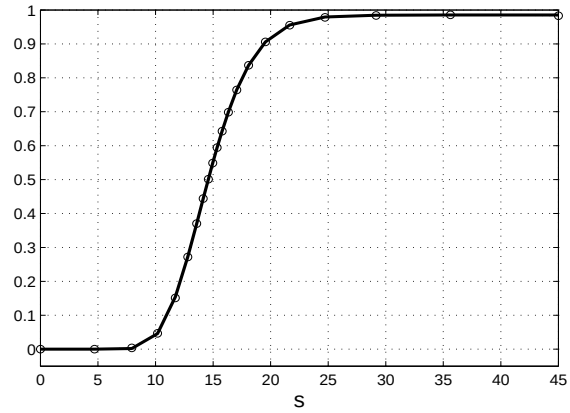

(c) $\Delta_h,\ \xi = 1$

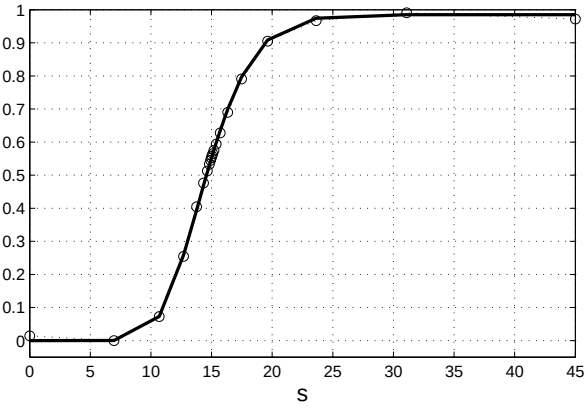

(d) $\Delta_h,\ \xi = 12$

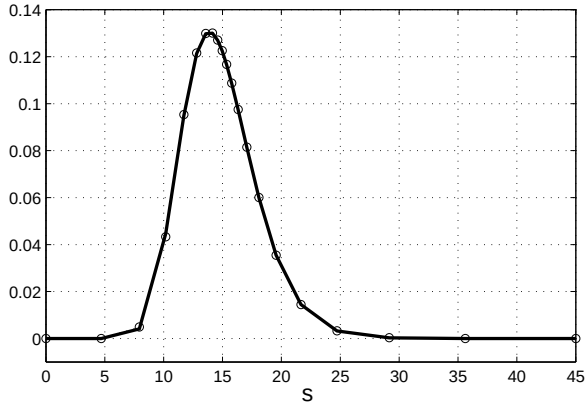

(e) $\Gamma_h,\ \xi = 1$

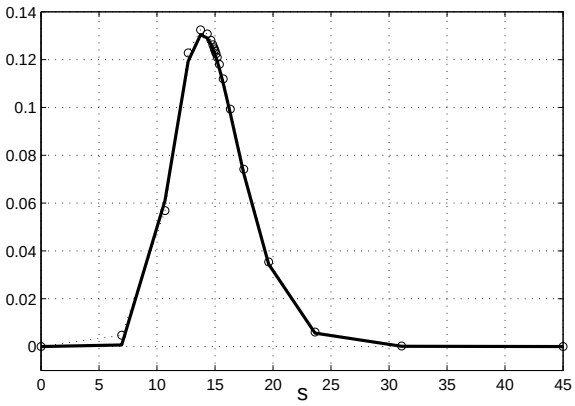

(f) $\Gamma_h,\ \xi = 12$

Fig. 3. Plots of numerical option price u_h, Δ_h and Γ_h of a European call, $K = 15, \sigma = 0.3, r_d = 0.03, r = 0.05, T = 0.5$, versus the analytic solution with the 20 points stretched grids.

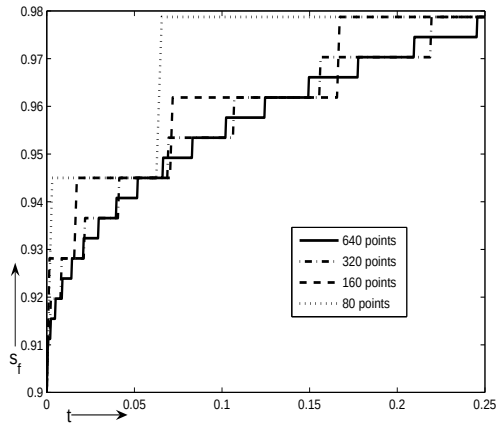

(a) equidistant grid $\sigma = 0.1$

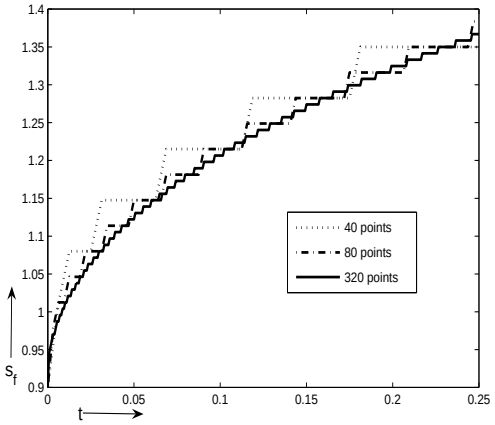

(b) equidistant grid $\sigma = 0.4$

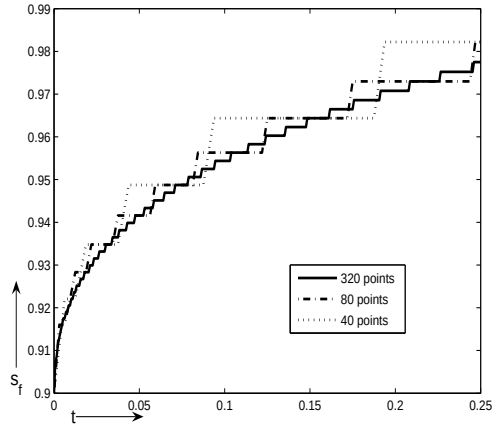

(c) FS-grid $\sigma = 0.1$

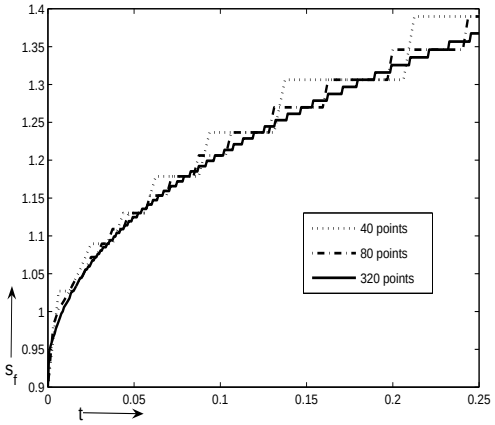

(d) FS-grid $\sigma = 0.4$

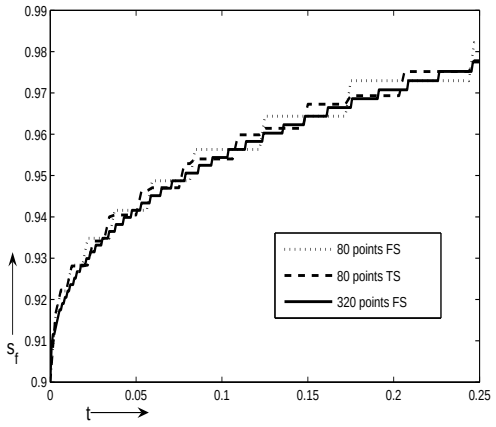

(e) TS-grid $\sigma = 0.1$

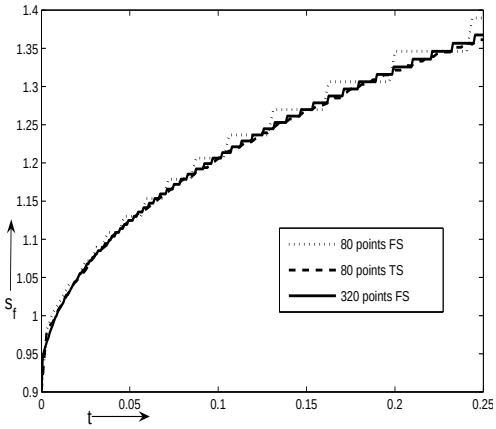

(f) TS-grid $\sigma = 0.4$

Fig. 4. The discrete free boundary s_f as a function of time to maturity t for different volatilities on equidistant and stretched grids. Parameters are $K = 0.9, r = 0.02, r_d = 0.035, T = 0.25$.

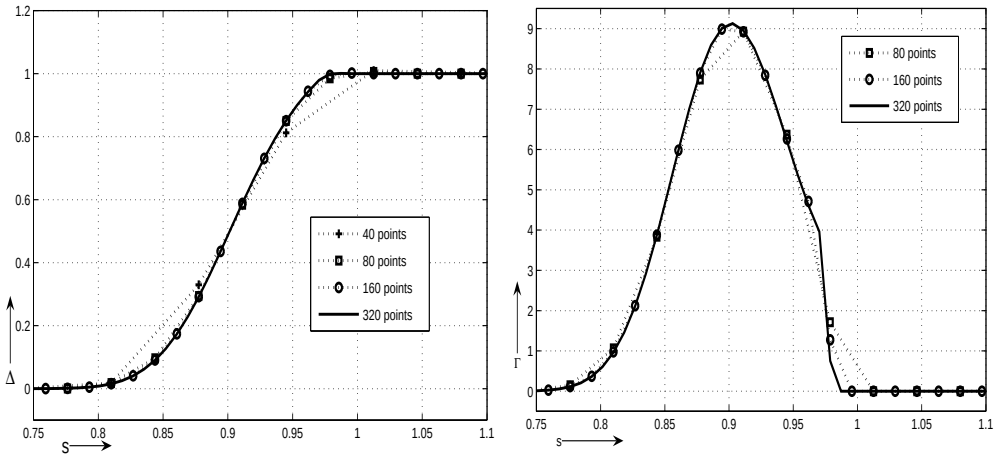

(a) Delta Δ (b) Gamma Γ

Fig. 5. Δ_h and Γ_h for an American call on *equidistant grids* of different resolution (in the right figure the 40 points curve is omitted). Parameters are $K = 0.9, \sigma = 0.1, r = 0.02, r_d = 0.035, T = 0.25$.

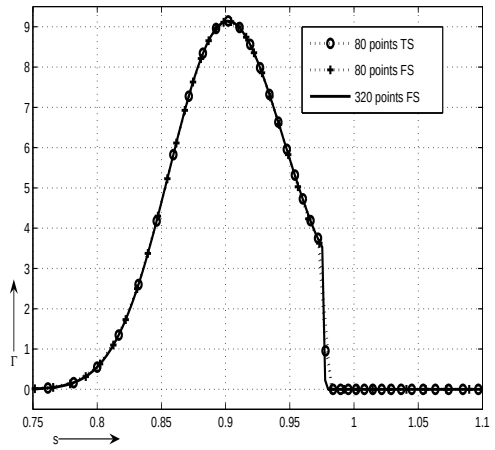

(a) Γ_h; $\sigma = 0.1$

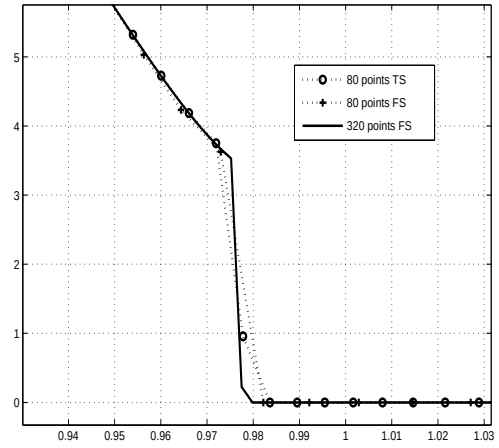

(b) Zoom of Γ_h; $\sigma = 0.1$

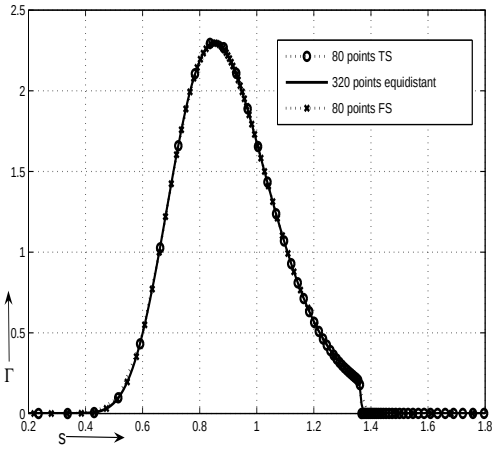

(c) Γ_h; $\sigma = 0.4$

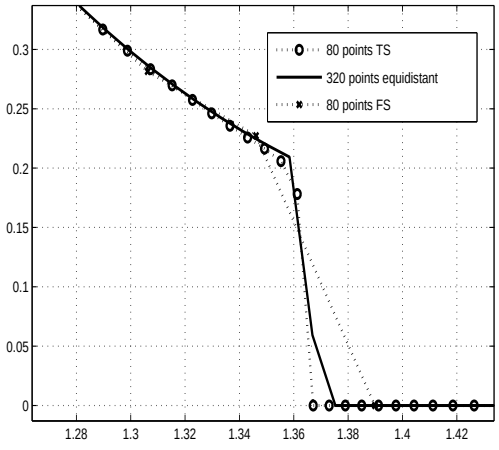

(d) Zoom of Γ_h; $\sigma = 0.4$

Fig. 6. Comparison of Γ_h near the early exercise boundary for an American call obtained with FS and TS for different σ. $\xi = 16$ for both schemes. Other parameters are $K = 0.9, r = 0.02, r_d = 0.035, T = 0.25$.

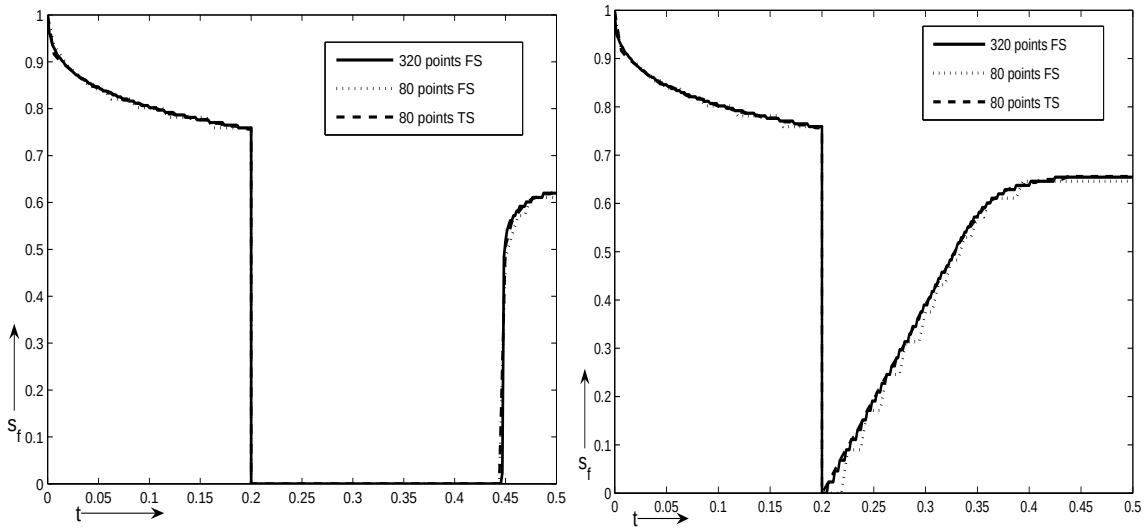

(a) discrete dividend $D = 0.02$ (b) proportional dividend $\rho = 0.02$

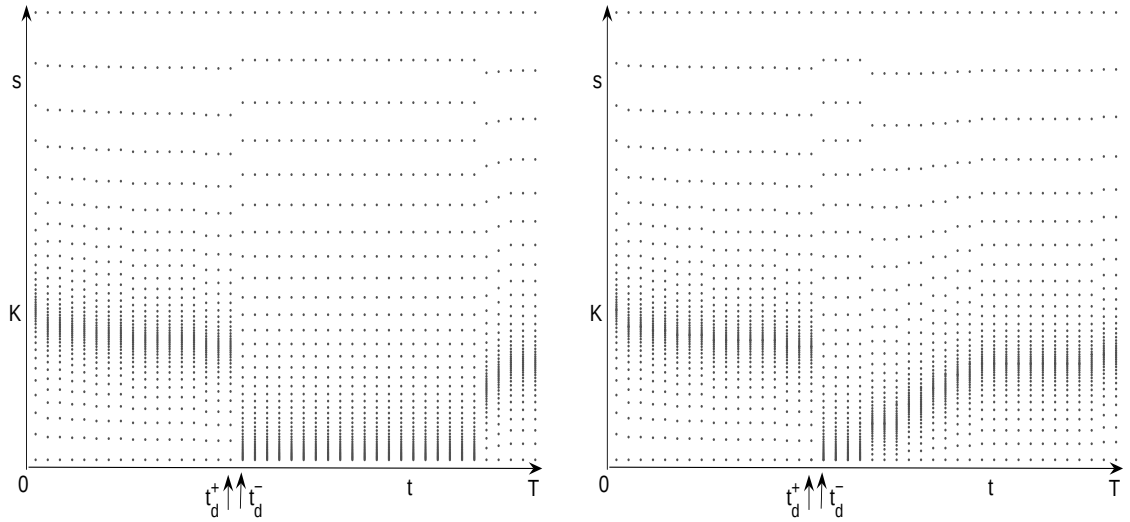

(c) grid for fixed dividend amount (d) grid for fixed dividend rate

Fig. 7. The free boundary s_f of an American put with a discrete and a proportional dividend payment plus the corresponding time-dependent grids. Parameters are $K = 1, \sigma = 0.4, r = 0.08, T = 0.5, t_d = 0.3$.

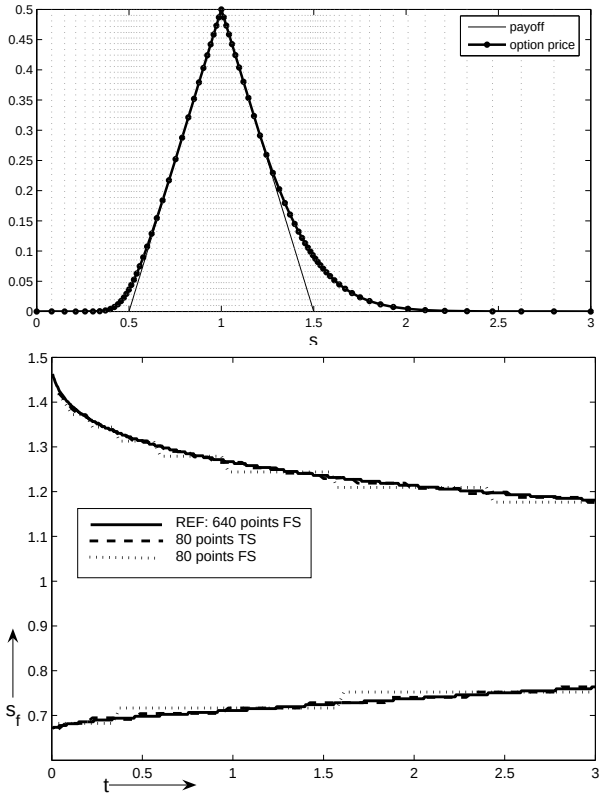

Fig. 8. American butterfly spread price (left) and free boundaries s_f as functions of time to maturity t (right picture). Parameters are $K_1 = 0.5, K_2 = 1.5, \sigma = 0.1, r = 0.02, r_d = 0.015, T = 3$.